

## Comparision of $Zn_2TiO_4$ and rutile $TiO_2$ photocatalysts for $H_2$ production under UV and near-visible light irradiation

Pramod H.Borse<sup>a</sup>, C. R. Cho<sup>b</sup>, K. T. Lim<sup>c</sup>, T. E. Hong<sup>d</sup>, E. D. Jeong<sup>d</sup>, J. H. Yoon<sup>d</sup>, S. M. Yu<sup>d</sup> and H. G. Kim<sup>d,\*</sup>

<sup>a</sup>Centre for Nanomaterials, International Advanced Research Centre for Powder Metallurgy and New Materials, Balapur P.O., Hyderabad, AP, India

<sup>b</sup>Department of Nano Fusion Technology, Pusan National University, Pusan 609-735, Korea

<sup>c</sup>Department of Imaging System Engineering, Pukyong National University, Busan 609-735, Korea

<sup>d</sup>Busan Center, Korea Basic Science Institute, Busan 609-735, Korea

$Zn_2TiO_4$  a spinel-type structure photocatalyst, was synthesized by a solid-state reaction method, and obtained as a single phase in the temperature range of 900-1200 °C. The average particle size for case of the as-synthesized  $Zn_2TiO_4$  sample, sintered at 1200 °C was found to be 5 μm, whereas it lay in the range of 0.5-2 μm for the case of  $TiO_2$  calcined at 650 °C. The band gap of  $Zn_2TiO_4$  and  $TiO_2$  (rutile) samples determined by UV-Vis diffuse reflectance spectra (DRS) was 3.10 eV (400 nm). The  $Zn_2TiO_4$  sample calcined at 1200 °C exhibited a higher hydrogen production rate than that of rutile  $TiO_2$  from a water-methanol mixture under UV ( $\lambda \geq 210$  nm) and near-visible ( $\mu \geq 400$  nm) light irradiation. In spite of having the same bandgap energy, the photocatalytic activity of  $Zn_2TiO_4$  was found to be higher than that of rutile  $TiO_2$ , manly because of its more negative conduction band edge than rutile  $TiO_2$ .

**Key words:**  $Zn_2TiO_4$ , Rutile  $TiO_2$ , Photocatalysis, Hydrogen production, Visible light.

### Introduction

Photocatalysts convert solar energy into useful chemical energy, such as hydrogen gas [1-3] as an alternative green fuel. Thus production of hydrogen by making use of semiconductor photocatalysts, has recently received much attention [4-7]. In general, to develop a high efficiency photocatalyst for hydrogen production, the semiconductor material should fulfill various requirements, such as (i) a proper band gap position; (ii) bandgap energy; (iii) long-term stability, (iv) good optical property etc. According to Matsumoto [8],  $Zn_2TiO_4$  is a fascinating candidate having an ideal bandgap energy (ca. 3.1 eV), as well as the band positions for photo-reduction of water under UV and near-visible light. Interestingly its band gap (ca. 3.1 eV) [9] is the same as rutile  $TiO_2$ . In spite of such a similarity, to the best of our knowledge, there is no report on comparison of the photocatalytic activities of the two systems. It can be predicted that the photocatalytic activity of rutile  $TiO_2$  may be lower than the activity of  $Zn_2TiO_4$ , as the conduction band edge of rutile  $TiO_2$  is located very near to the reduction potential of hydrogen [8]. In this paper we have carried out a comparative study of photocatalytic properties of  $Zn_2TiO_4$  and rutile  $TiO_2$  systems under UV and near-visible light irradiation.

Here, we synthesized  $Zn_2TiO_4$  by a solid-state reaction method, and  $TiO_2$  by a sol-gel process. Further structural and optical characterization was carried out with an objective of a photocatalytic application of these systems. A detailed study was carried out to compare the photocatalytic activity of the two materials for hydrogen production from a water-methanol mixture under UV/near-visible light irradiation. In addition, a direct comparison of the computed electronic structures of the two systems is a salient feature of the present work.

### Experimental

$Zn_2TiO_4$  samples were synthesized by a conventional solid-state reaction (SSR) method. Stoichiometric amounts of ZnO (99.9%, Aldrich) and  $TiO_2$  (99%, Aldrich) were mixed and ground in methanol. The pelletized powders were calcined at 700-1300 °C for 4 h in a static furnace. On the other hand, for the purpose of comparison, an amorphous  $TiO_2$  precursor (ATP) sample was also prepared by a sol-gel method (SGM) [10]. Thus 10 ml of titanium isopropoxide  $Ti(OCH(CH_3)_2)_4$  (97.0%, Aldrich) was dissolved in 50 ml of ethyl alcohol and then 3 ml of aqueous ammonium hydroxide solution were added. A homogeneous sol or colloidal solution was obtained after a few hours of vigorous stirring.  $TiO_2$  nanoparticles with anatase and rutile phase structure were formed by heating these ATP samples in air at various temperatures in the range of 300-650 °C for 4 h in an electric furnace.

The  $Zn_2TiO_4$  and  $TiO_2$  samples prepared by the con-

\*Corresponding author:  
Tel : +82-51-974-6104  
Fax: +82-51-974-6116  
E-mail: hhgkim@kbsi.re.kr

ventional SSR methods were characterized by an X-ray diffractometer (Mac Science Co., M18XHF). X-ray diffraction (XRD) results were compared with the Joint Committee Powder Diffraction Standards (JCPDS) data for phase identification. The band gap energy and optical properties of the as-prepared materials was measured by a UV-visible diffuse reflectance spectrometer (Shimadzu, UV 2401). The morphology was determined by scanning electron microscopy (SEM, Hitachi, S-2460N) and high-resolution transmission electron microscopy (HR-TEM, Philips, CM 200).

The electronic band-structure calculation of  $Zn_2TiO_4$  was performed using the WIEN 97 package based on the full potential linearized augmented plane wave method [11]. This method uses the generalized gradient approximation, an improvement to the local spin-density approximation within density functional theory that is known to be an efficient and accurate scheme for solving the many-electron problem of a crystal. The crystallographic parameters for the calculation including lattice parameters and atomic positions were adopted from the literature [12].

The photo-reduction reactions of water were carried out at room temperature in an upper-irradiation type Pyrex reaction vessel hooked up into a closed gas circulation system. Photocatalytic reduction was carried out by irradiating suspended powders using a Hg-arc lamp (500W) equipped with a UV-visible light irradiation. The  $H_2$  evolution was examined in an aqueous methanol solution (distilled water 80 ml and  $CH_3OH$  20 ml) by stirring 0.3 g of the catalyst loaded with 0.2 wt% Pt. Before photocatalytic reactions, all the catalysts were loaded with 0.2 wt% Pt using conventional impregnation method using aqueous  $PtCl_2$ . The concentration of the reaction product ( $H_2$ ) was determined by a gas chromatograph equipped with a thermal conductivity detector (a molecular sieve 5-Å column and Ar carrier).

## Results and Discussion

Structural characterization of  $Zn_2TiO_4$  and  $TiO_2$  samples were carried out to compare the crystallization behaviors of the samples prepared at various calcination temperatures. Fig. 1 shows the XRD patterns of  $Zn_2TiO_4$  samples prepared by sintering the mixed precursor ( $ZnO$  and  $TiO_2$ ) at various temperatures. The samples formed above 800 °C exhibited an inverse spinel  $Zn_2TiO_4$  structure with a lattice constant of 8.48 Å, and space group Fd3m [13]. The sample calcined at low temperatures (700 °C) showed some unknown impurity phases. The formation of  $Zn_2TiO_4$  was observed in the samples calcined between 800 and 1300 °C. The study clearly reveals the temperature-dependent crystallization behavior of  $Zn_2TiO_4$ .

Further, the structural characterization of  $TiO_2$  was studied in detail as seen in Fig. 2. Here, the X-ray patterns show the crystallization behavior of  $TiO_2$  as a function of the calcination temperature for the amorphous  $TiO_2$  precursor (ATP) sample. The  $TiO_2$  precursor sample did not show

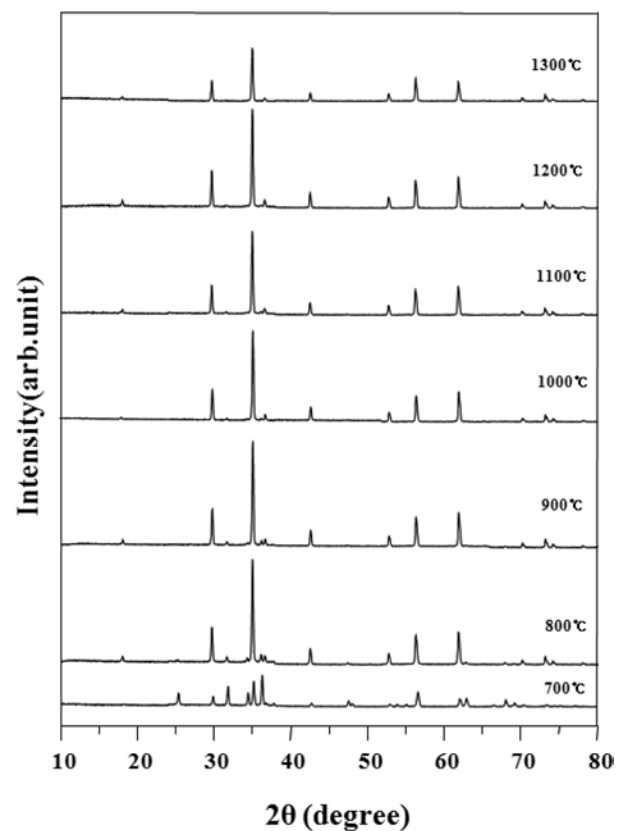


**Fig. 1.** XRD patterns of  $Zn_2TiO_4$  samples sintered at various temperatures for 4 h; (a) 700 °C, (b) 800 °C, (c) 900 °C, (d) 1000 °C , (e) 1100 °C , (f) 1200 °C , (g) 1300 °C .

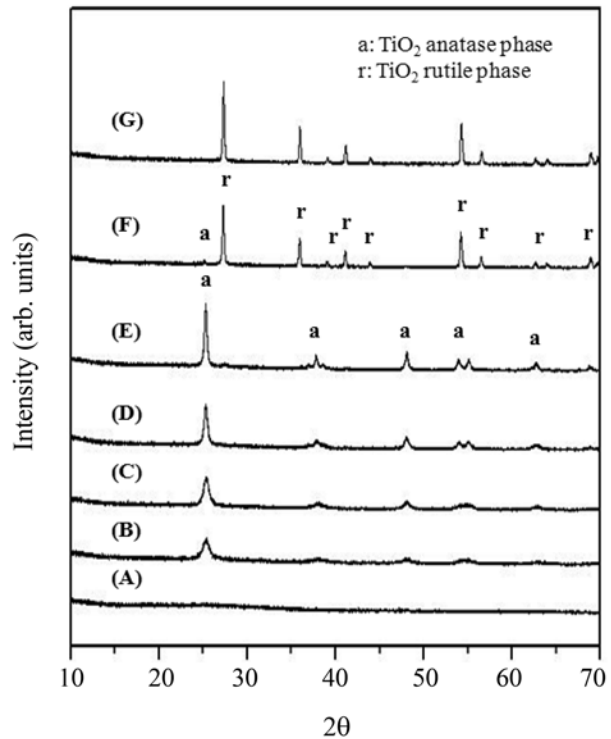
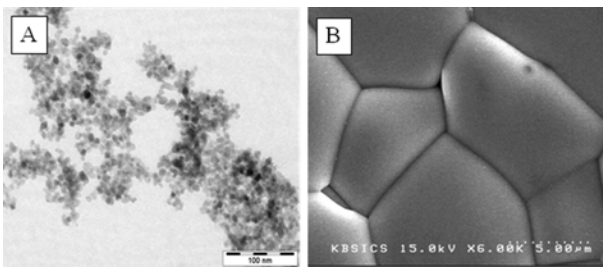


**Fig. 2.** XRD patterns of  $TiO_2$  samples calcined at various temperatures for 4 h; (A) 300 °C, (B) 350 °C, (C) 400 °C, (D) 450 °C , (E) 500 °C , (F) 550 °C , (G) 650 °C .

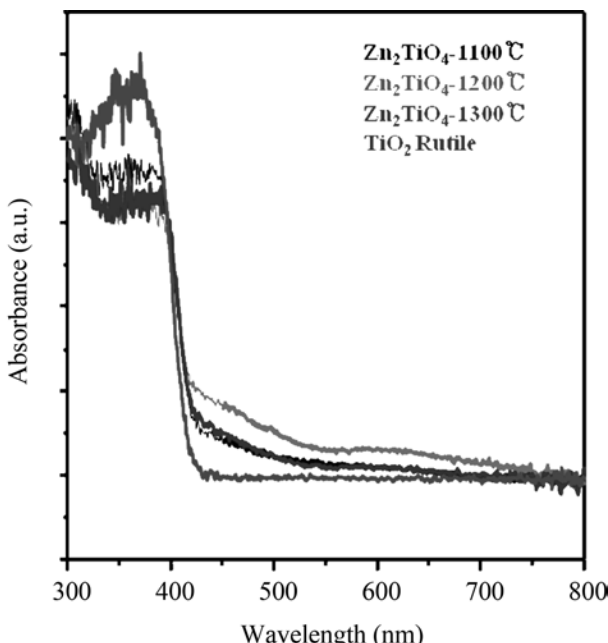
(Fig. 2(A)) any XRD peaks indicating that it was amorphous solid. Crystalline  $\text{TiO}_2$  grew with an increase in the calcination temperature. The crystallization behavior of  $\text{TiO}_2$  in the ATP sample was very similar to our previous report [10] and showed a well-crystallized anatase phase at 500 °C. But at higher temperatures ( $\geq 550$  °C) it turned to the thermodynamically more stable rutile phase.

Fig. 3 shows scanning electron microscopy (SEM) images of  $\text{TiO}_2$  and  $\text{Zn}_2\text{TiO}_4$  samples. The  $\text{TiO}_2$  sample displayed the existence of more or less spherical particles with a size range of 0.5–2  $\mu\text{m}$ . In contrast, the  $\text{Zn}_2\text{TiO}_4$  sample displayed a well-crystallized morphology with the grain size lying in the 5–10  $\mu\text{m}$  size range. Such larger particles are expected due to the high temperature-induced particle growth in this metal oxide.

Fig. 4 shows UV-vis diffuse reflectance spectra of  $\text{Zn}_2\text{TiO}_4$  samples sintered at different temperatures (1100, 1200, 1300 °C) and for a  $\text{TiO}_2$  (rutile) sample. Fig. 4 clearly indicates a similarity in the absorption edge of these systems.



**Fig. 3.** SEM images of (A)  $\text{TiO}_2$  calcined at 650 °C for 4 h; and (B)  $\text{Zn}_2\text{TiO}_4$  sample calcined at 1200 °C for 4 h.



**Fig. 4.** UV-Vis diffuse reflectance spectra of various samples of (a)  $\text{Zn}_2\text{TiO}_4$ -1100 °C, (b)  $\text{Zn}_2\text{TiO}_4$ -1200 °C, (c)  $\text{Zn}_2\text{TiO}_4$ -1300 °C and (d)  $\text{TiO}_2$ -650 °C indicating the similarity in the band gap of these systems.

From these spectra, we estimated the band gap energy of these materials.  $\text{TiO}_2$  (rutile) showed a sharp edge at 400 nm, while  $\text{Zn}_2\text{TiO}_4$  showed two absorption edges; the main edge at 400 nm and a shoulder around 400–500 nm. Thus, it can be concluded that both  $\text{Zn}_2\text{TiO}_4$  and  $\text{TiO}_2$  display a similar band gap of  $\sim 3.10$  eV, This is also shown in Table 1.

Fig. 5 shows the total density of states (DOS) for  $\text{Zn}_2\text{TiO}_4$  and rutile  $\text{TiO}_2$ , where the top of the valence band was set to 0 eV. The muffin-tin radii for Zn, Ti, and O were chosen to be 2.2, 2.0, and 1.8, respectively, in this calculation. The convergence parameter of  $R\text{Kmax}$  was set to 8.0. The calculation was iterated with a charge convergence criteria of 0.0001. The atomic coordinates for the WIEN97 calculation were adopted from the literature [14]. Similarly, the DOS was calculated for rutile  $\text{TiO}_2$ . Fig. 5 give a direct qualitative comparison of the DOS of these systems. Specifically DOS of  $\text{Zn}_2\text{TiO}_4$  implies

**Table 1.** Photocatalytic  $\text{H}_2$  production from methanol-water solution over 0.2 wt% Pt/ $\text{ZnTiO}_4$  and 0.2 wt% Pt/ $\text{TiO}_2$  samples

Catalyst	Bandgap Energy $E_g$ (eV)	H <sub>2</sub> evolution (mmol/gcat·h)	
		UV light irradiation ( $\lambda \geq 10$ nm)	Visible light irradiation ( $\lambda \geq 400$ nm)
0.2 wt% Pt/ $\text{Zn}_2\text{TiO}_4$ (1200 °C)	3.10	140	46
0.2 wt% Pt/ $\text{TiO}_2$ (650 °C)	3.10	11	2

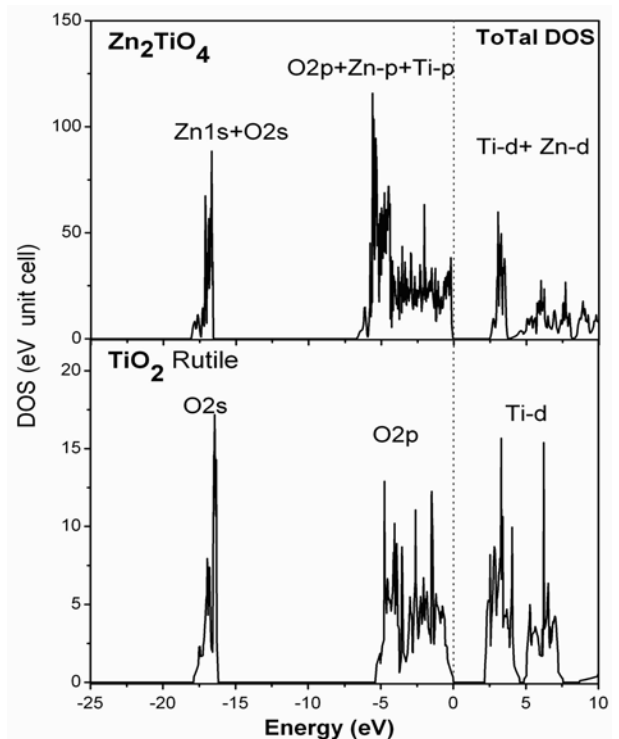


**Fig. 5.** Theoretically calculated total density of states (DOS) for  $\text{Zn}_2\text{TiO}_4$  and rutile  $\text{TiO}_2$ . The top of the valence band was set to 0 eV.

that the valence band is a mixture of the O 2p, Zn 2p and Ti 2p orbitals. The conduction band is comprised of the Zn 3d orbital. It is clear that titania also exhibits a similar DOS, except for the fact that there is no effect of the Zn-states in the conduction band. Effectively, the Zn states affect the conduction band edge position of  $Zn_2TiO_4$  making it a better photocatalyst. From the above study, it can be understood that both oxide systems show very similar optical properties.

Among the as-synthesized samples, we investigated the photocatalytic hydrogen production from a methanol-water solution using  $Zn_2TiO_4$  and rutile  $TiO_2$  samples under UV ( $\lambda \geq 210$ ) and visible ( $\lambda \geq 400$  nm) light irradiation. Table 1 shows the results of the  $H_2$  evolution as well as the respective band gaps of the samples calculated from the respective spectra. Two samples showed photocatalytic activity for hydrogen production from a methanol-water solution under UV light irradiation ( $\lambda \geq 210$ ). The  $Zn_2TiO_4$  photocatalyst showed a higher photocatalytic activity than that of rutile  $TiO_2$  under both UV and visible light irradiation. The  $Zn_2TiO_4$  photocatalyst showed a  $H_2$  production as high as 46 mmol/gcat·h under visible light irradiation ( $\lambda \geq 400$  nm). But, the rutile  $TiO_2$  photocatalyst showed a trace amount of  $H_2$  production.

The photocatalytic quantum yield (QY) of any photocatalyst is an important parameter to understand and compare its efficacy. It can be calculated using the following equation [15, 16]:

$$QY = H_2 \text{ evolution rate} / 14.757 \times [(I_1 - I_3) - (I_1 - I_2)] \times A_1 / A_2 \times 100 \quad (1)$$

where  $I_1$  is the blank light intensity,  $I_2$  is the scattered light intensity,  $I_3$  is the photocatalyst light intensity,  $A_1$  is the lighted area of the photo reactor,  $A_2$  is the area of the sensor face, and 14.757 is the mole number of photons with  $\lambda \geq 400$  nm emitted from the lamp for 1 h. The results of the photocatalytic QY calculation in Table 1, indicate that  $Zn_2TiO_4$  system shows 23 times more QY than rutile  $TiO_2$  system. This is an important observation of the present investigation.

Fig. 6 shows the bandgap positions of  $Zn_2TiO_4$  and rutile  $TiO_2$  photocatalysts reported by Matsumoto [8] and its mechanism for photocatalytic hydrogen production from a methanol-water solution. Although the two samples have the same bandgap energy, the conduction band of  $Zn_2TiO_4$  is located at a more negative position than that of rutile  $TiO_2$  as shown in Fig. 6(A). That is, in the case of Pt/ $Zn_2TiO_4$ , an electron excited to the conduction band has a reduction potential more suited to reduce an  $H^+$  ion, and a hole in the valence band also has a lower oxidation potential for  $CH_3OH$  degradation to  $CO_2$ . The figure clearly demonstrates this fact for  $Zn_2TiO_4$  and further compares it with the case of rutile  $TiO_2$  [17]. Therefore,  $Zn_2TiO_4$  is a potential photocatalyst for photocatalytic reactions which require a higher reduction potential as well as a lower oxidation potential.

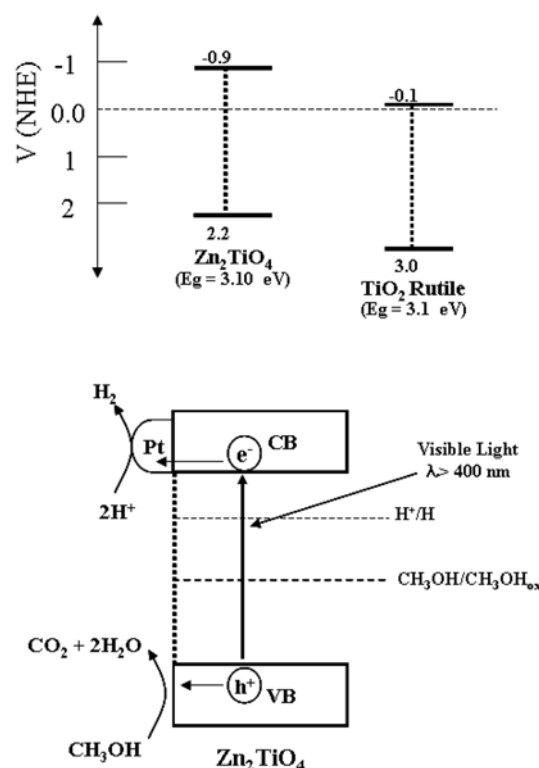


**Fig. 6.** A. The bandgap positions of  $Zn_2TiO_4$  and rutile  $TiO_2$  photocatalysts. B. The mechanism for photocatalytic hydrogen production from a methanol-water solution.

## Conclusions

Spinel-type zinc ferrite material,  $Zn_2TiO_4$  was successfully synthesized by a solid state reaction method and studied together with rutile  $TiO_2$  made by a sol-gel synthesis. In spite of having the same bandgap energy, the photocatalytic activity for hydrogen production under UV and near-visible light over  $Zn_2TiO_4$  was found to be higher than that of rutile  $TiO_2$ . Comparatively a more negative conduction edge position of  $Zn_2TiO_4$  than rutile  $TiO_2$  is mainly responsible for this better behavior of the Zn-containing system. Thus,  $Zn_2TiO_4$  can be considered as a better candidate for photocatalytic reactions which require a higher reduction potential as well as a lower oxidation potential viz. for photocatalytic hydrogen production.

## Acknowledgements

The authors acknowledge the support of KBSI grant T30320, Hydrogen Energy R&D Center, Korea. One of the authors (PB) acknowledges the support of Director ARCI, (DST lab) Hyderabad, India.

## Reference

1. J.S. Lee, Catal. Surv. Asia, 9 (2005) 217-227.
2. A. Kudo and Y. Miseki, Chem. Soc. Rev. 38 (2009) 253-259.
3. F.E. Osterloh, Chem. Mater. 20 (2008) 35-54.

4. H.G. Kim, D.W. Hwang and J.S. Lee, *J. Am. Chem. Soc.* 126 (2004) 8912-8913.
5. K. Maeda, T. Takata, M. Hara, N. Saito, Y. Inoue, H. Kobayashi and K. Domen, *J. Am. Chem. Soc.* 127 (2005) 8286-8287.
6. H.G. Kim, P.H. Borse, W. Choi and J.S. Lee, *Angew. Chem. Int. Ed.* 44 (2005) 4585-4589.
7. J.S. Jang, D.W. Hwang and J.S. Lee, *Catal. Today* 120 (2007) 174-184.
8. Y. Matsumoto, *J. Solid State Chem.* 126 (1996) 227-234.
9. T. Sreethawong, Y. Suzuki and S. Yoshikawa, *J. Solid State Chem.* 178 (2005) 329-338.
10. J.S. Jang, H.G. Kim, S.M. Ji, S.W. Bae, J.H. Jung, B.H. Shon and J.S. Lee, *J. Solid State Chem.* 179 (2006) 1067-1075.
11. P. Blaha, K. Schwarz and J. Luitz, WIEN97, A Full Potential Linearized Augmented Plane Wave Package for Calculating Crystal Properties, Techn. Universität Wien, Wien, Austria, (1999).
12. J.L. Shay and J.H. Wernick, *Ternary Chalcopyrite Semiconductor: Growth, Electronic Properties and Applications* (Pergamon, Oxford, 1974).
13. R.B. Rankin, A. Campos, H. Tian, R. Siriwardane, A. Roy, J.J. Spivey, D.S. Sholl and J.K. Johnson, *J. Am. Ceram. Soc.* 91 (2008) 584-590.
14. Chunfei Li, Y. Bando, M. Nakamura, N. Kimizuka and H. Kito, *Materials Research Bulletin* 35 (2000) 351-358.
15. B.W. Bae, P.H. Borse, S.J. Hong, J.S. Jang, J.S. Lee, E.D. Jeong, T.E. Hong, J.H. Yoon and H.G. Kim, *J. Korean Phys. Soc.* 51 (2007) S22-S26.
16. D.W. Hwang, H.G. Kim, J.S. Lee, J. Kim, W. Li and S.H. Oh, *J. Phys. Chem. B* 109, (2005) 2093-2102.
17. A. Fujishima, K. Hashimoto and T. Watanabe, *TiO<sub>2</sub> Photocatalysis: Fundamentals and Applications* (BKC, Inc.: Tokyo, 1999), p. 126.